PHILOSOPHICAL TRANSACTIONS OF THE ROYAL SOCIETY A

rsta.royalsocietypublishing.org

Review

**Cite this article:** Wang YJ, Gao JQ, Li MH, Shen Y, Hasanyan D, Li JF, Viehland D. 2014 A review on equivalent magnetic noise of magnetoelectric laminate sensors. *Phil. Trans. R. Soc. A* **372**: 20120455. http://dx.doi.org/10.1098/rsta.2012.0455

One contribution of 10 to a Theme Issue 'Magnetoelectric phenomena and devices'.

**Subject Areas:**
solid state physics, materials science

**Keywords:**
magnetoelectric effect, equivalent magnetic noise, magnetic field sensor, laminate composites, piezoelectric, magnetostrictive

**Author for correspondence:**
Y. J. Wang
e-mail: yaojin@vt.edu

Royal Society Publishing

# A review on equivalent magnetic noise of magnetoelectric laminate sensors

Y. J. Wang, J. Q. Gao, M. H. Li, Y. Shen, D. Hasanyan, J. F. Li and D. Viehland

Department of Materials Science and Engineering, Virginia Tech, Blacksburg, VA 24060, USA

Since the turn of the millennium, multi-phase magnetoelectric (ME) composites have been subject to attention and development, and giant ME effects have been found in laminate composites of piezoelectric and magnetostrictive layers. From an application perspective, the practical usefulness of a magnetic sensor is determined not only by the output signal of the sensor in response to an incident magnetic field, but also by the equivalent magnetic noise generated in the absence of such an incident field. Here, a short review of developments in equivalent magnetic noise reduction for ME sensors is presented. This review focuses on internal noise, the analysis of the noise contributions and a summary of noise reduction strategies. Furthermore, external vibration noise is also discussed. The review concludes with an outlook on future possibilities and scientific challenges in the field of ME magnetic sensors.

## 1. Introduction

Multiferroic materials, as a result of a coupling between dual order parameters, exhibit unusual physical properties and in turn promise new device applications. Of particular interest is the existence of a cross-coupling between the magnetic and electric orders, termed the magnetoelectric (ME) effect [1]. The ME coupling enables the control of the ferroelectric polarization by a magnetic field, and conversely the manipulation of magnetization by an electric field: in turn, producing two most promising scenarios—magnetic field sensors that could replace conventional devices and electric-write magnetic-read memory devices that combine the best of

ferroelectric and magnetic random-access memories [2,3]. The ME effect was first observed as an intrinsic effect in some natural single-phase materials [4]. Up to now, over 10 different single-phase compound families have been widely studied as multiferroic ME materials, such as the well-known $BiFeO_3$ and rare-earth manganates [5,6]. However, a high inherent ME coupling, especially above room temperature, has not yet been found in single-phase materials because most multiferroic compounds have low Curie temperatures [1,7]. The difficulties associated with uniting electric and magnetic ordering in a single phase have been circumvented by forming multi-phase multiferroic composites of piezoelectric and magnetostrictive components that can be electromagnetically coupled by stress mediation [8].

In the past few years, multi-phase ME composites have been under intensive study experimentally and theoretically, motivated by potential applications as passive magnetic field sensors. Experimentally, various composites with different dimensional connectivities and geometric configurations (e.g. 0-3 type particle composites, 2-2 type laminate composites, and 2-1 or 3-1 type fibre composites) and with different material components (e.g. ferrites and $BaTiO_3$ or $Pb(Zr_xTi_{1-x})O_3$ (PZT), Terfenol-D or Metglas and PZT or $Pb(Mg_{1/3}Nb_{2/3})O_3$–$PbTiO_3$ (PMN-PT)) have been reported [2,9,10]. Theoretically, Harshe [11] and Bichurin *et al*. [12] employed an average-field method to predict the response in ME composites under both quasi-static and resonance conditions based on magnetostrictive and piezoelectric constitutive equations [11,12], which has been further developed by introducing demagnetization, shear-lag and geometry effects [13–15]. Nan *et al*. [16] calculated the response of the composites and predicted a giant ME effect using the Green's function technique. For 2-2 laminate composites, Dong *et al*. [17] proposed an equivalent-circuit approach to model the ME coupling.

Experimental and theoretical progress concerning ME coefficients of multi-phase materials has been summarized and reviewed in a series of conference proceedings and especially in recent review articles [1,7,18]. The ME coefficient has been shown to be an important parameter, which can relate the ME coupling of various types of laminate configurations. However, the practical usefulness of a magnetic sensor is determined not only by the output signal of the sensor in response to an incident magnetic field, but also by the equivalent magnetic noise generated in the absence of such an incident field [19]. Here, we focus on recent progress in the equivalent magnetic noise reduction of ME magnetostrictive/piezoelectric laminate sensors, with an emphasis on the intrinsic noise floor. We try to summarize the progress that has been achieved and discuss the issues that remain to be addressed in the future.

## 2. Equivalent magnetic noise contributions

The detection capabilities of ME laminated sensors are affected by intrinsic and extrinsic noise. Extrinsic noise sources exist in the environment (examples include vibration and thermal noise), which can often be reduced or eliminated by rejection techniques [20]. However, it is not possible to reject intrinsic noise sources, such as Johnson noise and $1/f$ noise in the resistors and the semiconductors in detection circuits. Accordingly, measurement circuitry and laminate design must both be considered for ME sensor performance optimization [21,22].

The ME coupling coefficient is the parameter determining the detection capability for an ME sensor, including the ME voltage coefficient $\alpha_E$, which presents the relationship between the output electric field and the input magnetic one, and the ME charge coefficient $\alpha_Q$, which is used to characterize the charge generation capability of the sensor in response to an applied magnetic field. Correspondingly, either voltage or charge modes can be employed to amplify a small signal sensed by the ME laminate [23]. Here, we focus on the charge mode circuit, which is built around a low-noise operational amplifier, as it is more suitable for multi-push–pull mode Metglas/piezofibre sensors.

Figure 1 shows a schematic for a charge mode measurement circuit, including various noise sources. The ME sensor can be modelled as an $H$-induced charge generator, where $H$ is the applied magnetic field, in parallel with a capacitor $C$ and a resistor $R$, which together represent

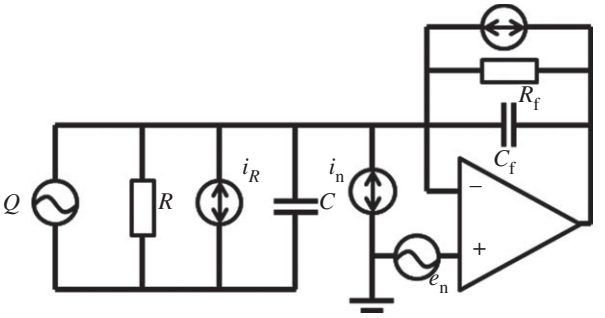


**Figure 1.** Basic detection circuit and noise model for an ME sensor [21,24].

the equivalent sensor parameters. Thus, for ME composites, there are two kinds of noise source, namely dielectric loss noise ($N_{\text{loss}}$) and leakage resistance noise ($N_R$). The noise charge density ($\text{C Hz}^{-1/2}$) for the ME composite part can be expressed as [19,24,25]

$$N_{\text{loss}} = \sqrt{\frac{4kTC\tan\delta}{2\pi f}} \tag{2.1}$$

and

$$N_R = \frac{1}{2\pi f}\sqrt{\frac{4kT}{R}}, \tag{2.2}$$

where $k$ is Boltzmann's constant ($1.38 \times 10^{-23}\,\text{J K}^{-1}$), $T$ is the temperature in kelvin, $\tan\delta$ is the dielectric loss and $f$ is the frequency in hertz.

In the circuit, a large feedback resistor $R_f$ was used in parallel with a feedback capacitor $C_f$ in order to obtain a sufficiently large output voltage, which produced a thermal noise ($N_{R_f}$). A low-noise amplifier was used in the circuit, which mainly generates current ($N_i$) and voltage ($N_e$) noise, as shown in figure 1. In addition, the transfer function ($\text{V pC}^{-1}$) is another important factor for an ME sensor, because a higher transfer function can improve the signal-to-noise ratio [21,26]. For the circuit in figure 1, the transfer function can be written as [24]

$$H_1(s) = \frac{1}{C_f}\frac{\text{i}2\pi f R_f C_f}{1 + \text{i}2\pi f R_f C_f}. \tag{2.3}$$

The noise charge density ($\text{C Hz}^{-1/2}$) for the circuit part can then be expressed as [24]

$$\left.\begin{aligned} N_{R_f} &= \frac{1}{2\pi f}\sqrt{\frac{4kT}{R_f}}, \\ N_i &= \frac{1}{2\pi f} i_n \\ \text{and}\quad N_v &= \frac{e_n|1 + Z/Z_f|}{|H(s)|}, \end{aligned}\right\} \tag{2.4}$$

where $i_n$ is the current noise density and $e_n = (e_{n,1\,\text{Hz}} - e_{n,1\,\text{kHz}})/f + e_{n,1\,\text{kHz}}$ is the voltage noise density of the low-noise amplifier. Finally, $Z = R/(1 + \text{i}2\pi f C R)$ and $Z_f = R_f/(1 + \text{i}2\pi f C_f R_f)$ represent the ME laminate and the feedback impedances, respectively.

Thus, the total noise charge density ($\text{C Hz}^{-1/2}$) can be obtained as

$$\text{noise charge density}\ (\text{C Hz}^{-1/2}) = \sqrt{N_R^2 + N_{\text{loss}}^2 + N_{R_f}^2 + N_i^2 + N_v^2}, \tag{2.5}$$

and the equivalent magnetic noise ($\text{T Hz}^{-1/2}$) can then be written as

$$\text{equivalent magnetic noise}\ (\text{T Hz}^{-1/2}) = \frac{1}{\alpha_Q}\sqrt{N_R^2 + N_{\text{loss}}^2 + N_{R_f}^2 + N_i^2 + N_v^2}. \tag{2.6}$$

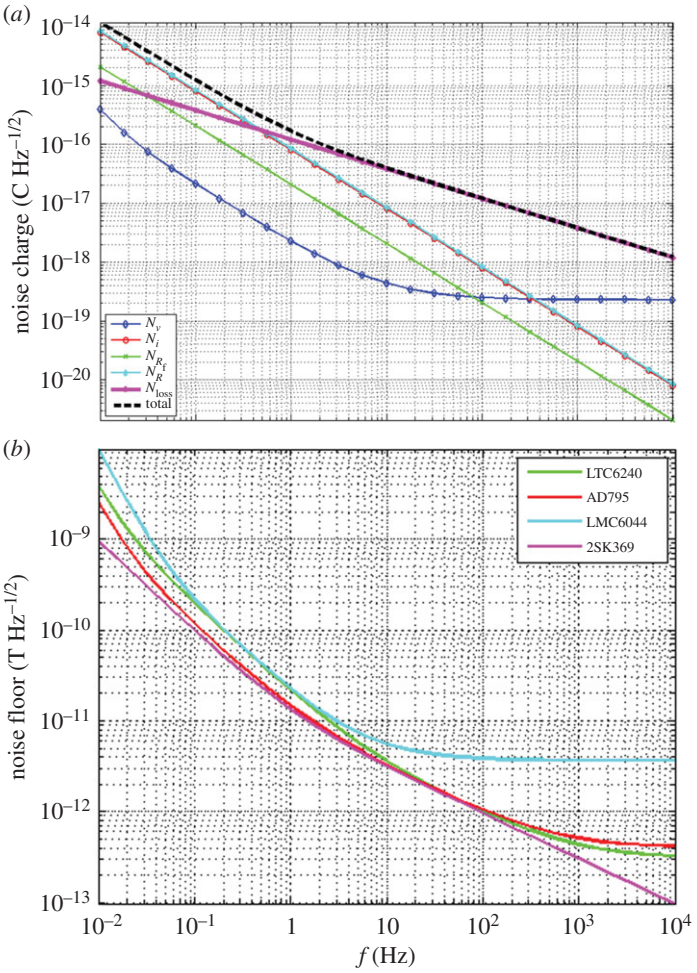


**Figure 2.** (*a*) Noise contributions of a sensor unit, consisting a Metglas/PZT-fibre laminate and based charge amplifier. (*b*) Equivalent magnetic noises of ME sensor units, consisting of a Metglas/PZT-fibre laminate and various low-noise amplifiers.

**Table 1.** The properties for a multi-push–pull mode Metglas/PZT sensor.

| composites | $C$ (pF) | $R$ (GΩ) | tan $\delta$ (%) | $\alpha_Q$ (C T$^{-1}$) |
|---|---|---|---|---|
| Metglas/PZT | 450 | 60 | 1.2 | $1250 \times 10^{-5}$ |

From equation (2.6), we can see the strategies that might be employed to reduce the equivalent magnetic noise of an ME sensor, including: (i) reducing the charge amplifier noise (via low-noise detection methods); (ii) reducing ME laminate noise (via reducing dielectric loss and increasing DC resistance of piezoelectric phase); (iii) increasing the charge coefficient without introducing additional noise (via increasing the piezomagnetic coefficient of magnetostrictive materials); and (iv) increasing the charge coefficient (via sensor arrays).

In order to analyse the contributions from the various noise sources, the noise charge density of a multi-push–pull mode Metglas/PZT sensor can be estimated, as shown in figure 2*a*. The properties of the sensor and the parameters for a junction field-effect transistor (JFET) low-noise amplifier are listed in tables 1 and 2, respectively. From this figure, we can see that all the noise sources contribute to the total noise floor. The contribution of each noise source was significantly dependent on frequency. At an interesting frequency of $f = 1$ Hz, the total noise charge density

**Table 2.** Circuit components used for charge amplifier.

| Op-amp[a] | $e_{n,1\,Hz}$ (nV Hz$^{-1/2}$) | $e_{n,1\,kHz}$ (nV Hz$^{-1/2}$) | $i_n$ (fA Hz$^{-1/2}$) | $R_f$ (GΩ) | $C_f$ (pF) |
|---|---|---|---|---|---|
| AD795 | 90 | 11 | 0.6 | 200 | 10 |
| LTC6240 | 52 | 7 | 0.6 | 10 | 100 |
| LMC6040 | 220 | 83 | 0.2 | 10 | 100 |
| JFET 2SK369 | 5 | 0.5 | 0.6 | 1000 | 10 |

[a]Cited from SAIC DARPA reports.

was dominated by the ME laminate noise (i.e. dielectric loss noise $N_{loss}$). The noise contributions from the circuit were much smaller, which is the reason why the electric circuit noise was ignored in some previous publications [19,25,27].

## 3. Intrinsic equivalent magnetic noise

Progress in the equivalent magnetic noise reduction of ME magnetostrictive/piezoelectric laminate sensors has been made in the past few years. In particular, a 1 Hz equivalent magnetic noise of 5.1 pT Hz$^{-1/2}$ has been obtained, which is lower than that of commercial flux-gate sensors, and even close to that of the optically pumped ultralow magnetic field sensors [28]. Here, we first focus on the strategies that have been employed to reduce the intrinsic equivalent magnetic noise of ME sensors. The circuit noise of various low-noise op-amps has been discussed, and the investigations revealed that a JFET amplifier had the lowest noise floor at $f = 1$ Hz. Both the interfacial bonding between interdigitated (ID) electrodes and piezofibre and the poling process of piezofibre are important to the properties of ME sensors, especially to the dielectric loss: accordingly, the interfacial bonding and poling process have been optimized [29–31]. Magnetic flux concentrators have been used to enhance the flux density, and in turn to enhance the effective ME coefficient [32,33]. These can be employed to reduce the equivalent magnetic noise via an increase in the signal gain without the introduction of additional noise sources [33]. Stressed magnetostrictive materials have a higher piezomagnetic coefficient, and in turn stress can be used to reduce the equivalent magnetic noise via enhancing the ME charge coefficient [34,35]. Single-crystal piezoelectrics, for example lead magnesium niobate–lead titanate (PMN-PT) single crystals, exhibit ultrahigh piezoelectric coefficients of approximately 2000 pC N$^{-1}$ and low $\tan\delta$ value of approximately 0.005. Thus, PMN-PT single crystals provide opportunities for realization of higher magnetic field sensitivity through a combination of giant ME effects and ultralow equivalent magnetic noise [19,25,36,37]. Finally, the ME output signal can be $N$ times enhanced if $N$ sensors are stacked together [38], which provides a strategy to reduce the equivalent magnetic noise by sensor stacking.

### (a) Low-noise amplifier

In an effort to reduce the electronic noise from the detection circuits, several different charge amplifiers have been designed based on various op-amps, listed in table 2. Figure 2*b* shows a comparison of the electrical noise spectra of an AD795-based charge amplifier to that of an LMC6044-based one. The results reveal a significant reduction in the spectral noise density at 1 Hz and above. The improvement is primarily due to the use of the lower noise, higher voltage op-amps in the first stage of the circuit and the larger feedback resistors.

### (b) Interfacial bonding optimization

A multi-push–pull mode ME heterostructure was composed of piezoelectric PZT fibres, ID electrodes and magnetostrictive Metglas foils [29], in which the thickness of the Stycast epoxy

**Table 3.** Poling procedures for PMN-PT fibres and their properties poled under various procedures [30].

| poling procedures | $T$ (°C) | $E_1$ (V mm$^{-1}$) | $E_2$ (V mm$^{-1}$) | Ramp up/down (V min$^{-1}$) | $\varepsilon_r$ | tan $\delta$ (%) | $d_{33}$ (pC N$^{-1}$) | $k_{33}$ (%) |
|---|---|---|---|---|---|---|---|---|
| a | 25 | 1000 | 0 | 100 | 3850 | 2.1 | 920 | 0.74 |
| b | 25 | 1000 | 0 | 20 | 3890 | 1.7 | 980 | 0.76 |
| c | 120 | 1000 | 500 | 100 | 3980 | 1.6 | 1140 | 0.83 |
| d | 120 | 1000 | 500 | 20 | 3950 | 1.1 | 1280 | 0.85 |

layer between the ID electrodes and PZT fibres determines the interfacial bonding region. To optimize the interfacial bonding, three PZT-fibre core composites were fabricated, denoted as sensors 1#, 2# and 3# [29]. These results demonstrate that improvement of the interfacial bonding condition between Kapton and PZT fibre layers results in an increase in $\alpha_E$ by a factor of 1.3 [29]. Moreover, the equivalent magnetic noise floor of sensor 1# was found to be lower than that of the other two over the entire bandwidth. The equivalent magnetic noise at 1 Hz for sensors 1#, 2# and 3# were $4.8 \times 10^{-11}$ T Hz$^{-1/2}$, $3.7 \times 10^{-11}$ T Hz$^{-1/2}$ and $2.7 \times 10^{-11}$ T Hz$^{-1/2}$, respectively. The findings demonstrate that an improved method of interfacial bonding can decrease the equivalent magnetic noise floor by a factor of approximately 2.

## (c) Poling optimization

For piezoelectric single crystals, the material properties are quite sensitive to the poling conditions [39], especially for the piezoelectric coefficient and dielectric loss [39], which are key parameters to the equivalent magnetic noise. Thus, the study of poling effects on ME sensors is technologically important. Four PMN-PT samples were all poled at an electric field of $E_1 = 1000$ V mm$^{-1}$, but at various temperatures and with different $E$-field ramp rates, as detailed in table 3. The dielectric constant of the PMN-PT fibre was found to be insensitive to voltage ramp rate and exhibited negligible enhancement when poled at higher temperatures. The values of $d_{33}$ and $k_{33}$ for PMN-PT were significantly enhanced after poling at an elevated temperature of $T = 120$°C, probably due to smaller domain sizes and more neutral domain-wall configurations. However, the values of tan $\delta$ decreased both with reduced voltage ramp rate and with increasing poling temperature [30].

After optimizing the poling conditions, two Metglas/PMN-PT sensors were poled following procedures (a) and (d). The maximum values of $\alpha_E$ for the two sensors were 31 V cm$^{-1}$ Oe$^{-1}$ and 42 V cm$^{-1}$ Oe$^{-1}$ [30]. These results demonstrate that optimal poling conditions result in an increase in $\alpha_E$ by a factor of 1.4. As reported in [30], the experimental equivalent magnetic noise at $f = 1$ Hz for the two sensor units poled following procedures (a) and (d) were 13 pT Hz$^{-1/2}$ and 8 pT Hz$^{-1/2}$, respectively. A reduction by a factor of 1.6 in the equivalent magnetic noise has been achieved solely by optimization of the poling conditions [30].

## (d) Geometry design

Magnetic flux concentration (MFC) can enhance the effective ME coefficient of an ME sensor, but meanwhile the large size of concentrators is opposite to the needs of device miniaturization [32]. In view of this point, ME laminate sensors with self-MFC effect were studied, including dumbbell-shaped and aspect ratio-based ME sensors [33,40,41].

A designed dumbbell-shaped sensor with an improved effective ME coefficient, and a reduced equivalent magnetic noise was reported [33], in which the dumbbell shape acts as a 'horn' to concentrate magnetic flux. The results demonstrated that ME laminates with symmetric dumbbell-shaped Metglas layers exhibited 1.5 times larger ME coefficients, 1.4 times lower

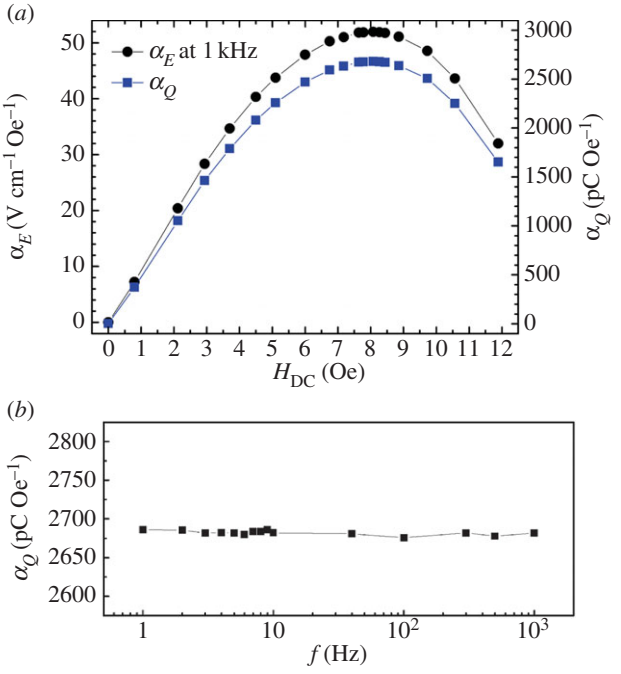


**Figure 3.** (*a*) The magnetic field dependence of $\alpha_E$ and $\alpha_Q$ of the Metglas/PMN-PT fibre sensor. (*b*) ME charge coefficient shows a flat response over the quasi-static frequency range [19].

**Table 4.** Property parameters for multi-push–pull mode Metglas/PMN-PT and L-T mode Metglas/Mn-doped PMN-PT sensors and the related pure single crystals [36].

| $\varepsilon_{33}$ | tan $\delta$ | $d_{33}$ or $d_{31}$ (pC N$^{-1}$) | $C$ (pC) | tan $\delta$ | $R_{DC}$ (G$\Omega$) | $\alpha_E$ (V cm$^{-1}$ Oe$^{-1}$) | $\alpha_Q$ (pC Oe$^{-1}$) |
|---|---|---|---|---|---|---|---|
| ⟨001⟩-PMN-PT[a] | | | | M-P-P mode Metglas/PMN-PT[c] | | | |
| 7000 | 0.005 | 2000 | 344 | 0.008 | 80 | 52 | 2680 |
| ⟨110⟩-Mn-doped PMN-PT[b] | | | | L-T mode Metglas/Mn-doped PMN-PT | | | |
| 1300 | 0.001 | 1800 | 3120 | 0.0014 | 10 | 61.5 | 3914 |

[a]Cited from Ceracomp Co., Ltd.
[b]Measured based on IEEE standards.
[c]Cited from [19].

required DC magnetic bias fields and 1.6 times higher magnetic field sensitivities than traditional rectangular-shaped ME laminates [33].

## (e) Single-crystal sensors

Piezoelectric single crystals, for example lead PMN-PT, exhibit ultrahigh piezoelectric coefficients of approximately 2000 pC N$^{-1}$ and low tangent losses of approximately 0.005. In particular, it has been found that Mn substitutions in PMN-PT are effective at achieving higher coercive fields, and lower dielectric permittivities and tangent losses, as summarized in table 4. The superior properties of Mn-doped PMN-PT single crystal provide opportunities for realization of higher magnetic field sensitivity through a combination of giant ME effects and an ultralow equivalent magnetic noise. Moreover, it has been reported that a single-crystal lanthanum gallium tantalite-based ME sensor also exhibits high ME coefficients and low equivalent magnetic noise due to a low dielectric constant and a high piezoelectric strain coefficient [10].

First, a multi-push–pull mode Metglas/PMN-PT sensor was reported. Figure 3 shows the ME coefficient as a function of $H_{DC}$ and frequency over the frequency range of $1\,\text{Hz} < f < 1\,\text{kHz}$. Under optimal DC magnetic bias ($H_{DC} \sim 8\,\text{Oe}$), $\alpha_E$ reached a maximum value of $52\,\text{V cm}^{-1}\,\text{Oe}^{-1}$, which is the highest ME coefficient yet reported [19]. The ME charge coefficient ($\alpha_Q$) is also presented in figure 3*a*. A maximum $\alpha_Q$ of $2680\,\text{pC Oe}^{-1}$ was obtained under a DC magnetic bias field of $H_{DC} \sim 8\,\text{Oe}$. Figure 3*b* shows $\alpha_Q$ as a function of frequency under the optimal $H_{DC} = 8\,\text{Oe}$. These results demonstrate that the high values of $\alpha_Q \sim 2680\,\text{pC Oe}^{-1}$ are maintained down to quasi-static frequencies. As discussed in §2, the charge noise density due to $\tan\delta$ and the DC resistance can be modelled based on equations (2.1) and (2.2). The predicted results reveal that both the $\tan\delta$ noise and DC resistance noise contributed to the total noise floor at 1 Hz, but the magnitude of the $\tan\delta$ noise was 1.2 times larger than that of the DC resistance noise. After the noise charge density has been measured, the equivalent magnetic noise spectra can be obtained through a conversion of the charge noise density spectrum using the ME charge coefficient (see [19]). An extremely low equivalent magnetic noise of $5.1\,\text{pT Hz}^{-1/2}$ was found at 1 Hz for the Metglas/PMN-PT sensors, which is very close to the predicted value of $4.2\,\text{pT Hz}^{-1/2}$. Please note that the equivalent magnetic noise of the ME sensor unit was as low as about $1\,\text{pT Hz}^{-1/2}$ at a frequency of only several hertz [19].

Mn-doped PMN-PT single crystals have the advantages of high $d_{31}$ and extremely low $\tan\delta$. Accordingly, an L-T mode Metglas/Mn-doped PMN-PT bimorph heterostructure has been studied and compared with a multi-push–pull mode Metglas/PMN-PT one [19,36]. The induced charge of such bimorph heterostructure for $N = 5$ (where $N$ is the number of Metglas layers) was investigated for $1\,\text{Hz} < f < 1\,\text{kHz}$ under $H_{AC} = 0.05\,\text{Oe}$ and $H_{DC} = 5\,\text{Oe}$. It can also be seen that $\alpha_Q$ was relatively insensitive to frequency for $1\,\text{Hz} < f < 70\,\text{Hz}$, i.e. $4087\,\text{pC Oe}^{-1}$ at 1 Hz, and $3948\,\text{pC Oe}^{-1}$ at 70 Hz [36].

The noise charge density is presented in figure 4*a*. For the multi-push–pull mode sensor, both $\tan\delta$ and $R_{DC}$ noise contributed notably to the total noise charge density at 1 Hz, but the magnitude of the $\tan\delta$ noise was 1.2 times larger than that of the $R_{DC}$ noise. However, for the L-T mode sensor, the total noise charge density at 1 Hz was dominated by the $R_{DC}$ noise, and the magnitude of the $R_{DC}$ noise was 45.5 times larger than that of the $\tan\delta$ noise. In figure 4*b*, the noise model predicts that the 1 Hz equivalent magnetic noise of the L-T mode is 1.3 times higher than that of multi-push–pull one (i.e. $5.5\,\text{pT Hz}^{-1/2}$ to $4.2\,\text{pT Hz}^{-1/2}$), whereas the 10 Hz value was 1.3 times lower (i.e. $0.8\,\text{pT Hz}^{-1/2}$ relative to $1.0\,\text{pT Hz}^{-1/2}$). Experimentally, an ultralow equivalent magnetic noise of $6.2\,\text{pT Hz}^{-1/2}$ was found at 1 Hz [36].

## 4. Extrinsic equivalent magnetic noise

As mentioned in §2, the equivalent magnetic noise of an ME sensor is impacted by both internal and external (or environmental) noise sources. Thermal fluctuations couple into the noise via the pyroelectric effect, and mechanical vibrations couple via the piezoelectric effect. These pose significant obstacles for practical application of ME sensors [42]. A symmetric Terfenol-D/PZT bimorph-laminated structure has presently been developed to reject thermal fluctuation noise [42]. Similarly, symmetric signal/unsymmetrical noise (SS-UN) and unsymmetrical signal/symmetric noise (US-SN) modes have been developed for Metglas/piezofibre ME laminates with the capability of vibrational noise rejection [20] (Y. Wang, J. Gao, M. Li, D. Hasanyan, Y. Shen, J. Li, D. Viehland 2012, unpublished data). More recently, a simple structure of Metglas/piezofibre ME laminates was found under mechanically clamped condition that can reduce vibration noise (Y. Wang, D. Hasanyan, Y. Shen, J. Li, D. Viehland 2012, unpublished data).

A laminate structure design based on the differential mode for vibrational noise cancellation has been reported [20]. Unlike other Metglas/PZT/Metglas sandwich structures, two layers of PZT, two single-sided and a double-sided Kapton ID electrodes were used to create a differential symmetric structure. In the design, the two PZT-fibre layers were poled along the same orientation. Owing to the symmetrical nature of the structure, the double-sided electrode in the middle acts as a neutral plane. Application of a magnetic field along the longitudinal

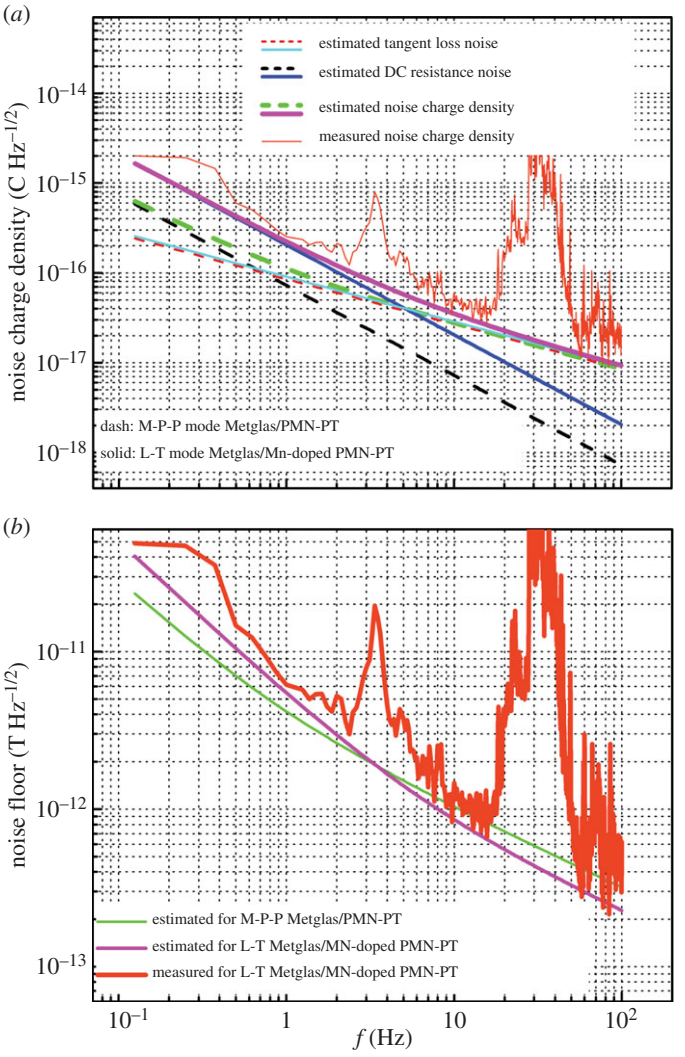


**Figure 4.** (*a*) Measured and estimated noise charge density and (*b*) equivalent magnetic noise for the multi-push–pull mode Metglas/PMN-PT sensor unit [19] and the proposed one over the frequency range of 0.125 Hz $< f <$ 100 Hz. The noise contributions, including constituent dielectric loss and DC resistance loss, are compared [36].

direction of the laminate will cause the sensor to contract or elongate longitudinally. Contraction or expansion in the plane of the sensor will result in an identical charge in each PZT layer. Parallel electrical connection of the PZT layers would therefore result in a doubling of the signal. Conversely, an applied external vibrational signal will tend to cause an asymmetric (bending mode) deformation. Simultaneous elongation of the top PZT and contraction of the bottom one will result in charges of opposite polarity in the PZT layers. Parallel electrical connection of the PZT, therefore, results in an attenuation of the output signal.

The response of each layer of the differential sensor, as well as the summation of the constituent signals, is presented in figure 5*a*. In this figure, the blue line shows the output signal from the top PZT layer, the red dashed line is the signal generated by the bottom PZT layer and the black dashed line is the time-domain summation of the top and bottom PZT layers. Figure 5*a* shows that the amplitude of the combined signal (black trace) is significantly attenuated relative to either of the two constituent output signals (red and blue traces). In order to analyse the data more accurately, the power spectral density (PSD) of each component signal and of the

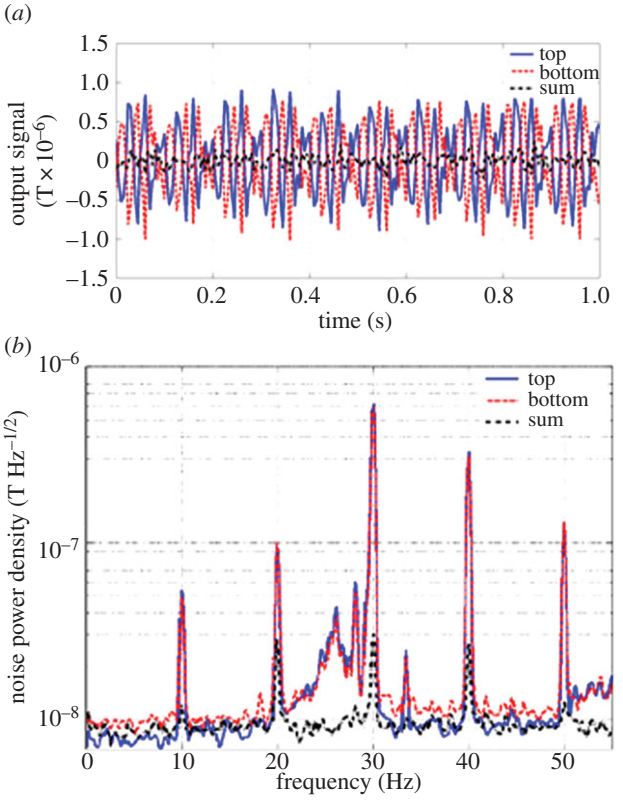


**Figure 5.** (*a*) Time-domain equivalent magnetic response of differential mode sensor to incident vibrational signal, and (*b*) PSD of top, bottom and time-domain summation of top and bottom [20].

time-domain summation of the two signals was calculated using MATLAB. Figure 5*b* shows the power density of the output signals of the top, bottom and time-domain summation over the frequency range from DC to 55 Hz. At the vibrational drive frequency of 10 Hz, the amplitude of the summation signal was five times smaller than either that of the top or bottom PZT layers ($10^{-8}\,\mathrm{T\,Hz^{-1/2}}$ versus $5 \times 10^{-8}\,\mathrm{T\,Hz^{-1/2}}$, respectively). In addition, the second, third, fourth and fifth harmonic signals (20, 30, 40 and 50 Hz) exhibited the same trends. The summation signal of the third harmonic was 10-fold attenuated. In fact, the differential structure ME sensor also shows the significant cancellation to the vibrational noise at frequency ranging from 10 Hz to hundreds of hertz [20].

## 5. Future directions

Future directions should include the following.

### (a) Extremely low-frequency equivalent magnetic noise

Besides the equivalent magnetic noise, another important consideration for the design of magnetic sensors is the frequency bandwidth of detectable magnetic fields. Some specific applications require extremely low-frequency detection. For example, magnetoencephalography measurements span a frequency range from about 10 mHz to 1 kHz [43]. However, most investigations have focused on the frequency bandwidth of $1\,\mathrm{Hz} < f < 1\,\mathrm{kHz}$ [19,36]. In order to study the extremely low-frequency response, both the charge amplifier and ME structure need

to be optimized [24]. Increased feedback resistors can help to reduce the noise of the charge amplifier. However, it is not easy to fabricate resistors with huge resistances and small tolerances.

## (b) Gradiometer

Gradiometry has carried over as an effective method to reduce environmental noise. It employs two (or more) magnetic sensors in a differential mode configuration. Such configurations are capable of rejecting common noise sources that are coherently shared between two sensors spatially separated by a baseline or sensor arrays [44].

The noise rejection efficiency of the gradiometer system is limited by internal incoherent noise sensors and difficulties between ME sensors, especially in phase responses. Thus, advances in reducing the equivalent magnetic noise floor and phase shift of individual ME sensors would be beneficial to ME gradiometer developments in the future.

## (c) Modulation techniques

Based on a nonlinear ME effect, it has been theoretically and experimentally established that a modulation–demodulation technique can be employed to enhance the magnetic field sensitivity at arbitrary frequencies [45,46]. A giant sharp ME resonance for an ME composite is important to this modulation technique [46]. Thus, constitutive components with high mechanical quality factor should be investigated and developed.

Acknowledgements. The authors greatly acknowledge the help of and discussion with Dr Keith McLaughlin in Science Applications International Corporation (SAIC) and Prof. Christophe Dolabdjian in Groupe de Recherche en Informatique, Image, Automatique et Instrumentation de Caen (GREYC). The authors also acknowledge Prof. Haosu Luo in Shanghai Institute of Ceramics, Chinese Academic of Science, for providing high-performance piezoelectric single crystals.

Funding statement. This work was sponsored by the Office of Naval Research.

# References

1. Nan CW, Bichurin MI, Dong SX, Viehland D, Srinivasan G. 2008 Multiferroic magnetoelectric composites: historical perspective, status, and future directions. *J. Appl. Phys.* **103**, 031101. (doi:10.1063/1.2836410)
2. Eerenstein W, Wiora M, Prieto JL, Scott JF, Mathur ND. 2007 Giant sharp and persistent converse magnetoelectric effects in multiferroic epitaxial heterostructures. *Nat. Mater.* **6**, 348–351. (doi:10.1038/nmat1886)
3. Wang YJ, Cheung KF, Or SW, Chan HLW, Luo HS. 2008 PMN-PT single crystal and Terfenol-D alloy magnetoelectric laminated composites for electromagnetic device applications. *J. Ceram. Soc. Jpn* **116**, 540–544. (doi:10.2109/jcersj2.116.540)
4. Fiebig M, Lottermoser T, Frohlich D, Goltsev AV, Pisarev RV. 2002 Observation of coupled magnetic and electric domains. *Nature* **419**, 818–820. (doi:10.1038/nature01077)
5. Valencia S *et al.* 2011 Interface-induced room-temperature multiferroicity in $BaTiO_3$. *Nat. Mater.* **10**, 753–758. (doi:10.1038/nmat3098)
6. Zhao T *et al.* 2006 Electrical control of antiferromagnetic domains in multiferroic $BiFeO_3$ films at room temperature. *Nat. Mater.* **5**, 823–829. (doi:10.1038/nmat1731)
7. Ma J, Hu J, Li Z, Nan C-W. 2011 Recent progress in multiferroic magnetoelectric composites: from bulk to thin films. *Adv. Mater.* **23**, 1062–1087. (doi:10.1002/adma.201003636)
8. Jin J, Lu S-G, Chanthad C, Zhang Q, Hague MA, Wang Q. 2011 Multiferroic polymer composites with greatly enhanced magnetoelectric effect under a low magnetic bias. *Adv. Mater.* **23**, 3853–3858. (doi:10.1002/adma.201101790)
9. Wang YJ, Or SW, Chan HLW, Zhao XY, Luo HS. 2008 Enhanced magnetoelectric effect in longitudinal–transverse mode Terfenol-D/$Pb(Mg_{1/3}Nb_{2/3})O_3$–$PbTiO_3$ laminate composites with optimal crystal cut. *J. Appl. Phys.* **103**, 124511. (doi:10.1063/1.2943267)
10. Sreenivasulu G, Fetisov LY, Fetisov YK, Srinivasan G. 2012 Piezoelectric single crystal langatate and ferromagnetic composites: studies on low-frequency and resonance magnetoelectric effects. *Appl. Phys. Lett.* **100**, 052901. (doi:10.1063/1.3679661)

11. Harshe G. 1991 Magnetoelectric effect in piezoelectric–magnetostrictive composites, PhD thesis, Pennsylvania State University, PA, USA.
12. Bichurin MI, Filippov DA, Petrov VM, Laletsin VM, Paddubnaya N, Srinivasan G. 2003 Resonance magnetoelectric effects in layered magnetostrictive–piezoelectric composites. *Phys. Rev. B* **68**, 132408. (doi:10.1103/PhysRevB.68.132408)
13. Chang C-M, Carman G. 2007 Modeling shear lag and demagnetization effects in magneto-electric laminate composites. *Phys. Rev. B* **76**, 134116. (doi:10.1103/PhysRevB.76.134116)
14. Wang Y, Hasanyan D, Li M, Gao J, Li J, Viehland D, Luo H. 2012 Theoretical model for geometry-dependent magnetoelectric effect in magnetostrictive/piezoelectric composites. *J. Appl. Phys.* **111**, 124513. (doi:10.1063/1.4729832)
15. Hasanyan D, Gao J, Wang Y, Viswan R, Li M, Shen Y, Li J, Viehland D. 2012 Theoretical and experimental investigation of magnetoelectric effect for bending–tension coupled modes in magnetostrictive–piezoelectric layered composites. *J. Appl. Phys.* **112**, 013908. (doi:10.1063/1.4732130)
16. Nan C, Li M, Huang J. 2001 Calculations of giant magnetoelectric effects in ferroic composites of rare-earth–iron alloys and ferroelectric polymers. *Phys. Rev. B* **63**, 144415. (doi:10.1103/PhysRevB.63.144415)
17. Dong SX, Li JF, Viehland D. 2003 Longitudinal and transverse magnetoelectric voltage coefficients of magnetostrictive/piezoelectric laminate composite: theory. *IEEE Trans. Ultrason. Ferroelectr. Freq. Control* **50**, 1253–1261. (doi:10.1109/TUFFC.2003.1244741)
18. Bichurin MI, Petrov VM, Averkin SV, Liverts E. 2010 Present status of theoretical modeling the magnetoelectric effect in magnetostrictive–piezoelectric nanostructures. Part I: Low frequency and electromechanical resonance ranges. *J. Appl. Phys.* **107**, 053904. (doi:10.1063/1.3313919)
19. Wang YJ, Gray D, Berry D, Gao JQ, Li MH, Li JF, Viehland D. 2011 An extremely low equivalent magnetic noise magnetoelectric sensor. *Adv. Mater.* **23**, 4111–4114. (doi:10.1002/adma.201100773)
20. Gao J, Zhai J, Shen Y, Shen L, Gray D, Li J, Finkel P, Viehland D. 2011 Differential-mode vibrational noise cancellation structure for Metglas/Pb(Zr,Ti)$O_3$ fiber magnetoelectric laminates. *IEEE Trans. Ultrason. Ferroelectr. Freq. Control* **58**, 1541–1544. (doi:10.1109/TUFFC.2011.1980)
21. Zhuang X, Sing MLC, Cordier C, Saez S, Dolabdjian C, Das J, Gao J, Li J, Viehland D. 2011 Analysis of noise in magnetoelectric thin-layer composites used as magnetic sensors. *IEEE Sens. J.* **11**, 2183–2188. (doi:10.1109/JSEN.2011.2114648)
22. Jiao J, Li L, Ren B, Guo H, Deng H, Di W, Zhao X, Jing W, Luo H. 2012 Parallel multilayer magnetoelectric composite based on $(1-x)$Pb($Mg_{1/3}Nb_{2/3}$)–$x$$PbTiO_3$ and Terfenol-D coupled with charge mode amplifier. *J. Appl. Phys.* **111**, 043909. (doi:10.1063/1.3681818)
23. Jahns R, Greve H, Woltermann E, Quandt E, Knoechel RH. 2011 Noise performance of magnetometers with resonant thin-film magnetoelectric sensors. *IEEE Trans. Instrum. Meas.* **60**, 2995–3001. (doi:10.1109/TIM.2011.2122410)
24. Gao J, Wang Y, Li M, Shen Y, Li J, Viehland D. 2012 Quasi-static ($f < 10^{-2}$ Hz) frequency response of magnetoelectric composites based magnetic sensor. *Mater. Lett.* **85**, 84–87. (doi:10.1016/j.matlet.2012.06.100)
25. Wang Y, Gray D, Berry D, Gao J, Li J, Viehland D, Luo H. 2011 Equivalent magnetic noise in magnetoelectric Metglas/Pb($Mg_{1/3}Nb_{2/3}$)$O_3$–$PbTiO_3$ laminate composites. *Phys. Status Solidi – Rapid Res. Lett.* **5**, 232–234. (doi:10.1002/pssr.201105170)
26. Xing ZP, Li JF, Viehland D. 2007 Modeling and the signal-to-noise ratio research of magnetoelectric sensors at low frequency. *Appl. Phys. Lett.* **91**, 142905. (doi:10.1063/1.2794435)
27. Li M, Gao J, Wang Y, Gray D, Li J, Viehland D. 2012 Enhancement in magnetic field sensitivity and reduction in equivalent magnetic noise by magnetoelectric laminate stacks. *J. Appl. Phys.* **111**, 104504. (doi:10.1063/1.4718441)
28. Clarke J, Koch RH. 1988 The impact of high-temperature superconductivity on SQUID magnetometers. *Science* **242**, 217–223. (doi:10.1126/science.242.4876.217)
29. Wang Y, Gray D, Berry D, Li M, Gao J, Li J, Viehland D. 2012 Influence of interfacial bonding condition on magnetoelectric properties in piezofiber/Metglas heterostructures. *J. Alloys Compds.* **513**, 242–244. (doi:10.1016/j.jallcom.2011.10.029)

30. Wang Y, Gray D, Gao J, Berry D, Li M, Li J, Viehland D, Luo H. 2012 Improvement of magnetoelectric properties in Metglas/Pb($Mg_{1/3}Nb_{2/3}$)$O_3$–$PbTiO_3$ laminates by poling optimization. *J. Alloys Compds.* **519**, 1–3. (doi:10.1016/j.jallcom.2011.12.093)
31. Li M, Berry D, Das J, Gray D, Li J, Viehland D, Davies P. 2011 Enhanced sensitivity and reduced noise floor in magnetoelectric laminate sensors by an improved lamination process. *J. Am. Ceram. Soc.* **94**, 3738–3741. (doi:10.1111/j.1551-2916.2011.04659.x)
32. Dong SX, Zhai JY, Li JF, Viehland D. 2006 Enhanced magnetoelectric effect in three-phase $MnZnFe_2O_4$/$Tb_{1-x}Dy_xFe_{2-y}$/Pb(Zr,Ti)$O_3$ composites. *J. Appl. Phys.* **100**, 124108. (doi:10.1063/1.2402968)
33. Wang Y, Gray D, Berry D, Li J, Viehland D. 2012 Self-amplified magnetoelectric properties in a dumbbell-shaped magnetostrictive/piezoelectric composite. *IEEE Trans. Ultrason. Ferroelectr. Freq. Control* **59**, 859–862. (doi:10.1109/TUFFC.2012.2270)
34. Wang Y, Hasanyan D, Li M, Gao J, Viswan R, Li J, Viehland D. 2012 Electric-field tuning of magnetoelectric properties in Metglas/piezofiber composites. *Phys. Status Solidi – Rapid Res. Lett.* **6**, 265–267. (doi:10.1002/pssr.201206159)
35. Li M, Wang Y, Gao J, Li J, Viehland D. 2012 Enhanced magnetoelectric effect in self-stressed multi-push–pull mode Metglas/Pb(Zr,Ti)$O_3$/Metglas laminates. *Appl. Phys. Lett.* **101**, 022908. (doi:10.1063/1.4737179)
36. Wang Y, Gao J, Li M, Hasanyan D, Shen Y, Li J, Viehland D, Luo H. 2012 Ultralow equivalent magnetic noise in a magnetoelectric Metglas/Mn-doped Pb($Mg_{1/3}Nb_{2/3}$)$O_3$–$PbTiO_3$ heterostructure. *Appl. Phys. Lett.* **101**, 022903. (doi:10.1063/1.4733963)
37. Gao J, Das J, Xing Z, Li J, Viehland D. 2010 Comparison of noise floor and sensitivity for different magnetoelectric laminates. *J. Appl. Phys.* **108**, 084509. (doi:10.1063/1.3486483)
38. Xing ZP, Zhai JY, Gao JQ, Li JF, Viehland D. 2009 Magnetic-field sensitivity enhancement by magnetoelectric sensor arrays. *IEEE Electron Device Lett.* **30**, 445–447. (doi:10.1109/LED.2009.2015342)
39. Xiang Y, Zhang R, Cao WW. 2011 Poling field versus piezoelectric property for $[001]_c$ oriented 91%Pb($Zn_{1/3}Nb_{2/3}$)$O_3$–9%$PbTiO_3$ single crystals. *J. Mater. Sci.* **46**, 1839–1843. (doi:10.1007/s10853-010-5009-z)
40. Gao J, Gray D, Shen Y, Li J, Viehland D. 2011 Enhanced dc magnetic field sensitivity by improved flux concentration in magnetoelectric laminates. *Appl. Phys. Lett.* **99**, 153502. (doi:10.1063/1.3650713)
41. Fang Z, Lu SG, Li F, Datta S, Zhang QM, El Tahchi M. 2009 Enhancing the magnetoelectric response of Metglas/polyvinylidene fluoride laminates by exploiting the flux concentration effect. *Appl. Phys. Lett.* **95**, 112903. (doi:10.1063/1.3231614)
42. Zhai JY, Xing ZP, Dong SX, Li JF, Viehland D. 2008 Thermal noise cancellation in symmetric magnetoelectric bimorph laminates. *Appl. Phys. Lett.* **93**, 072906. (doi:10.1063/1.2969794)
43. Vrba J, Robinson SE. 2001 Signal processing in magnetoencephalography. *Methods* **25**, 249–271. (doi:10.1006/meth.2001.1238)
44. Shen Y, McLaughlin KL, Gao J, Li M, Li J, Viehland D. 2012 Effective optimization of magnetic noise for a Metglas/Pb(Zr,Ti)$O_3$ magnetoelectric sensor array in an open environment. *Mater. Lett.* **91**, 307–310. (doi:10.1016/j.matlet.2012.10.003)
45. Jahns R, Greve H, Woltermann E, Quandt E, Knoechel R. 2012 Sensitivity enhancement of magnetoelectric sensors through frequency-conversion. *Sens. Actuators A – Phys.* **183**, 16–21. (doi:10.1016/j.sna.2012.05.049)
46. Zhuang X, Sing MLC, Cordier C, Saez S, Dolabdjian C, Shen L, Li JF, Li M, Viehland D. 2011 Evaluation of applied axial field modulation technique on ME sensor input equivalent magnetic noise rejection. *IEEE Sens. J.* **11**, 2266–2272. (doi:10.1109/JSEN.2011.2131647)